Appl. Phys. B 79, 245–248 (2004)
DOI: 10.1007/s00340-004-1540-4

Applied Physics B
Lasers and Optics

R. DAI
W. GONG
J. XU
X. REN
D. LIU✉

The edge technique as used in Brillouin lidar for remote sensing of the ocean

Department of Physics, Applied Optics Beijing Area Major Laboratory, Beijing Normal University, Beijing 100875, P.R. China

Received: 17 November 2003/Revised version: 16 March 2004
Published online: 28 May 2004 • © Springer-Verlag 2004

ABSTRACT A new approach to remote sensing of the ocean is proposed. It is based on a combination of Brillouin scattering, incoherent lidar techniques and high-resolution frequency discrimination via gas absorption cells. The results of theoretical and experimental research are given. This approach provides the capability of rapid real-time monitoring of sound-speed or temperature profiles both in the open ocean and in littoral zones with high resolution and high accuracy.

PACS 42.68.Wt; 42.79.Qx; 78.35.+c

1 Introduction

Lidar remote-sensing measurements for frequency shifts smaller than 1 GHz have numerous atmospheric and oceanic applications. For measuring such small frequency shifts, the use of atomic resonance filters (ARFs) is an important technique [1, 2]. The so-called edge technique has been shown to be the most powerful technique for remote sensing of the atmosphere [3–5]. The most commonly used atomic resonance filter is the iodine absorption cell [6, 7].

Brillouin scattering shows significant potential in lidar remote sensing of the ocean. It can be used to measure the speed of sound and the temperature of the seawater [8–12]. Brillouin-scattering techniques have an advantage in comparison with Raman scattering because the narrow Brillouin line width minimizes the effects of daylight and fluorescence [13]. On the other hand, high-resolution spectroscopy is needed for Brillouin scattering. Hirschberg and Byrne addressed the high-resolution problem by using a dual Fabry–Pérot etalon [9]. It is, in fact, analogous to the edge technique discussed in recent years. Liu et al. made measurements using a scanning Fabry–Pérot etalon [12]. However, a Fabry–Pérot etalon has a very limited solid angle for acceptance of the lidar return signal, which severely limits the capabilities of such an approach. The innovative idea of using a Fabry–Pérot etalon combined with a zone plate avoids the acceptance solid angle problem [13], but an appreciable fraction of the signal photons are lost in the higher orders of the Fabry–Pérot. For practical applications, a powerful pulsed laser with a repetition rate of 10–20 Hz is necessary as the source of the lidar system. If Brillouin scattering is measured by a scanned Fabry–Pérot etalon, a long scanning period (which may be several minutes) is needed to obtain enough samples and a real-time measurement could not be made.

So, a technique to perform real-time measurement of Brillouin scattering in water with high resolution and accuracy is very important, and the edge technique is ideal for achieving this purpose. Although the edge technique has been successfully used in remote sensing of the atmosphere, there is no report of its use in remote sensing of the ocean. A Brillouin lidar system for remote sensing of the ocean based on the edge technique is presented as follows.

2 Basic considerations

The fundamental theory of Brillouin scattering is well known [14, 15]. In brief, the Brillouin scattering consists of two inelastically scattered Lorentzians centered symmetrically at $\pm\nu_B$ with respect to the Rayleigh line that has no frequency shift (see Fig. 1). For water, the width (FWHM) of the Brillouin lines is approximately 0.5 GHz and ν_B is 7–8 GHz [14]. The principle of using the edge technique to measure the Brillouin scattering in water is shown schematically in Fig. 2. The basic idea of the edge technique is to locate a frequency-dependent backscattering line on a steep edge of a transmission line of an optical filter, so that a small frequency change gives a large signal change.

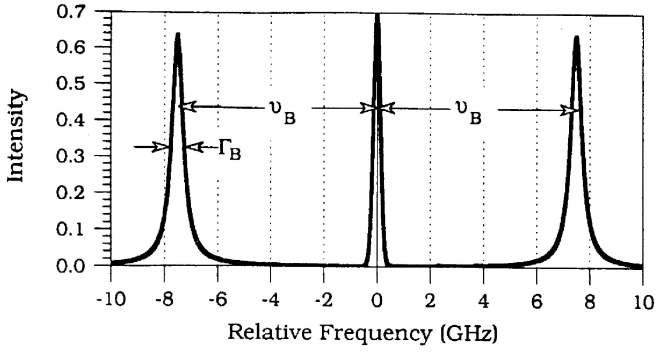

FIGURE 1 Ideal spectrum of Brillouin scattering in water

✉ Fax: +8610-62200141, E-mail: dhliu@bnu.edu.cn

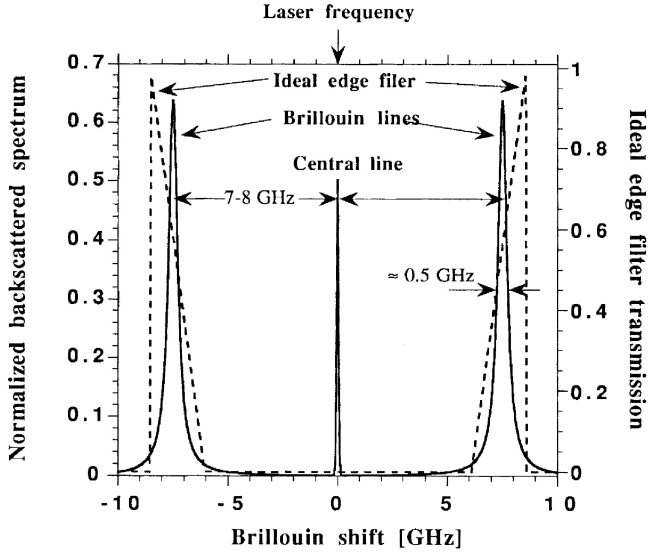

FIGURE 2 Principles of the edge technique

Based on the above, an ideal filter used in the edge technique should: (1) block the central line with the laser frequency; (2) have steep transmission edges located at the center of each Brillouin line with opposite slopes; (3) have a high maximum transmission and (4) reject the background light, i.e. have 100% absorption outside the transmission edge.

The edge technique has obvious advantages. Due to the steep slope of the edge a small change in the Brillouin shift will make a large change in the signal transmitted, so it is very sensitive and can achieve a high-resolution measurement. Another important advantage of such double edge filters is that a change in the incident laser frequency or a Doppler shift due to movements of the liquid will increase the edge-filter signal corresponding to one Brillouin line and decrease the signal corresponding to the other. Therefore, such systematic effects are canceled.

3 An example system using bromine and iodine absorption cells

Figure 3 shows an example of the system. The returned scattered signal first passes through a cell (called a blocker) containing an absorption gas, which absorbs the unshifted central frequency component and transmits most of the light in the Brillouin-shifted components. This transmitted signal then passes through a 1 : 1 beam splitter that sends one-half of the transmitted intensity to the first detector to form signal S_1; the remaining half passes through a second cell (edge filter) containing another absorbing gas and the intensity transmitted enters a second detector to form signal S_2. The fraction of the intensity absorbed in the second cell depends on the Brillouin shift due to the positions of its absorption lines.

The problem is to choose suitable absorption gases to match the frequency of the laser. There are many possible molecular transitions. In our system bromine and iodine are chosen since the Nd : YAG laser is generally used in remote sensing of the ocean. The first absorption cell (the blocker) is a Br_2 cell. Its absorption spectrum around the frequency of an Nd : YAG laser is shown in Fig. 4. The zero value of the frequency is $\nu_L = 18\,776.7402\,\mathrm{cm}^{-1}$, corresponding to a wavelength 532.573806 nm, which is well within the tuning range of an Nd : YAG laser. The second absorption cell (the edge filter) is an I_2 cell. Its absorption spectrum around the frequency of an Nd : YAG laser is shown in Fig. 5. The two absorption lines used are #1071 and #1073 corresponding to frequencies $18\,776.4607\,\mathrm{cm}^{-1}$ and $18\,777.0292\,\mathrm{cm}^{-1}$, respectively. To understand the function of the two cells the ideal spectrum of Brillouin scattering in water is shown in Figs. 4 and 5.

The profiles $g_{\mathrm{Br}}(\nu)$ and $g_{\mathrm{I}}(\nu)$ of the two spectra can be obtained by fitting the data of the two figures. Also, the Brillouin line is a Lorentzian, which is expressed as

$$f(\nu, \nu_{\mathrm{B}}) = \frac{1}{\pi\Gamma_{\mathrm{B}}}\left\{\frac{1}{1+[2(\nu-\nu_{\mathrm{B}})/\Gamma_{\mathrm{B}}]^2} + \frac{1}{1+[2(\nu+\nu_{\mathrm{B}})/\Gamma_{\mathrm{B}}]^2}\right\}, \quad (1)$$

where Γ_{B} is the width (FWHM) of the Brillouin lines, which has a typical value of $\Gamma_{\mathrm{B}} = 0.5$ GHz. Assuming that the signal intensity incident on the Br_2 cell (blocker) is unity, then, according to Fig. 3, the fractions of the lidar return that are received by the first and second detectors are given by

$$\varrho_1(\nu_{\mathrm{B}}) = \frac{1}{2}\int_{-\infty}^{\infty} f(\nu, \nu_{\mathrm{B}})\, g_{\mathrm{Br}}(\nu)\mathrm{d}\nu\,, \quad (2)$$

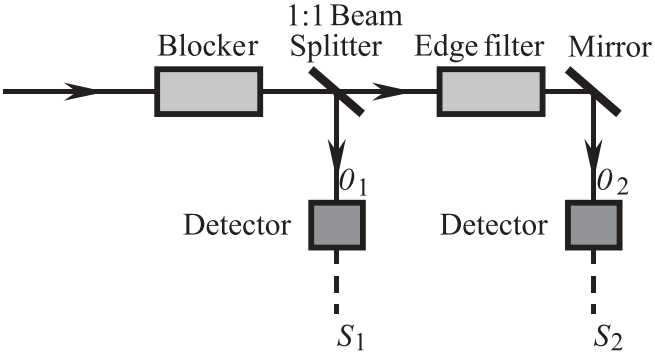

FIGURE 3 Schematic for an example system

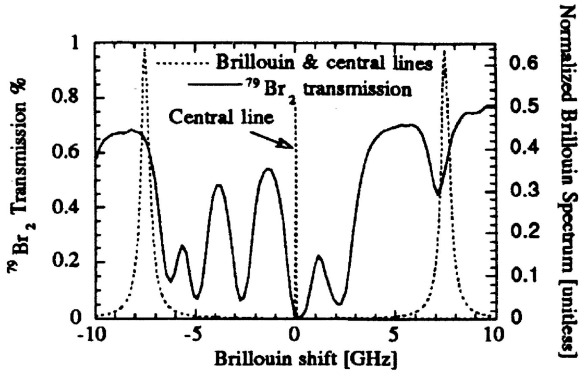

FIGURE 4 Absorption spectrum of a bromine ($^{79}Br_2$) cell

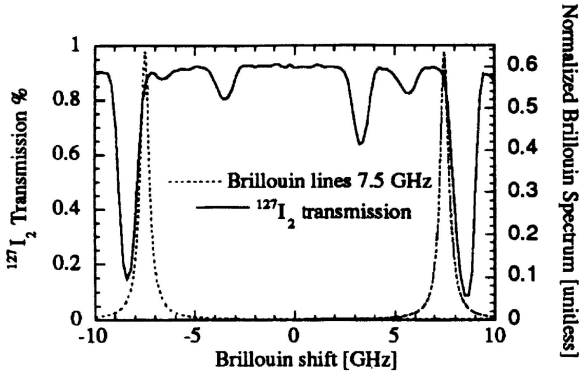

FIGURE 5 Absorption spectrum of an iodine ($^{127}I_2$) cell

$$\varrho_2(\nu_B) = \frac{1}{2}\int_{-\infty}^{\infty} f(\nu, \nu_B) g_{Br}(\nu) g_I(\nu) d\nu \,. \quad (3)$$

The observed signals are

$$S_1 = \varrho_1 N_{pe} \,, \quad S_2 = \varrho_2 N_{pe} \,, \quad (4)$$

where N_{pe} is the number of output Brillouin photo-electrons produced per pulse by an optical receiver in a pulsed laser backscattering system. A normalized signal intensity $S(\nu_B)$ can be defined as

$$S(\nu_B) = \frac{S_2}{S_1} = \frac{\varrho_2}{\varrho_1} \quad \text{or} \quad S(\nu_B) = \frac{S_2}{S_1 - S_2} = \frac{\varrho_2}{\varrho_1 - \varrho_2} \,. \quad (5)$$

The definition $S(\nu_B) = S_2/S_1$ will be used here. The Brillouin shift can be determined from the normalized intensity. Figure 6 gives the dependence of the Brillouin shift on the value of the normalized signal. It can be clearly seen that there is one-to-one correspondence between normalized intensity and Brillouin shift.

4 Experimental measurements

Figure 7 shows schematically the geometry of the set-up for taking experimental measurements. In our experiments an injection-seeded pulsed Nd : YAG laser (Continuum 9010) was employed, which was tuned so that its frequency

FIGURE 6 Brillouin-shift dependence of normalized intensity

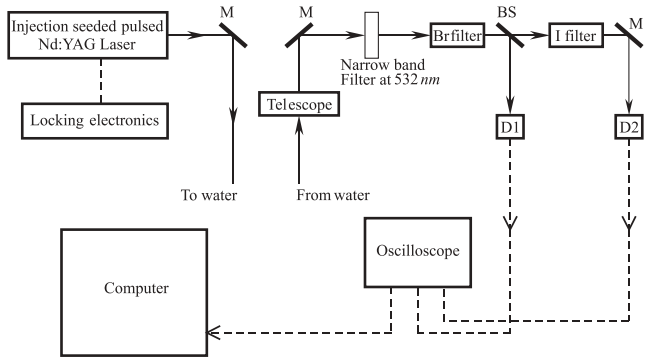

FIGURE 7 Set-up geometry of experimental measurements. M: mirror, BS: beam splitter. The narrow-band filter is a multiple-layer interference filter with a bandwidth of 3 nm and a transmission of 62%

matches the central frequency of the Br cell exactly. The oscilloscope used was an Agilent Infinium 54832B, and a command was used to measure the peak value. The software Agilent VEE was used for data acquisition and control of the oscilloscope. In the telescope we used a pinhole with a diameter of 15 μm to block the noise from other directions. A narrow-band filter with 3-nm bandwidth and 62% transmission was used to minimize the noise from other frequencies. The telescope, the narrow-band filter and the two absorption cells were aligned in a 3-m-long PVC tube. The scattered signal from the water was reflected into the tube by a curved mirror. The temperatures of the two absorption cells were controlled electronically so that proper absorption could be measured.

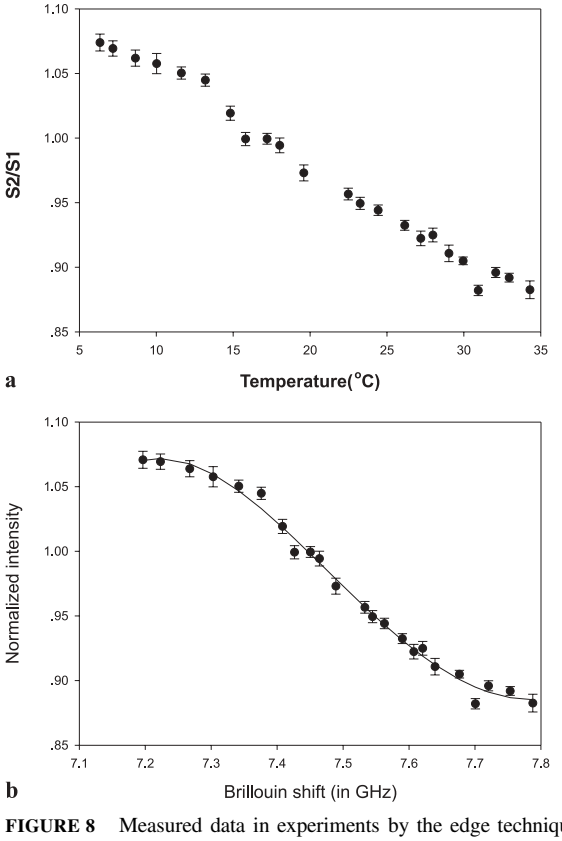

FIGURE 8 Measured data in experiments by the edge technique. **a** Temperature dependence of normalized signal, **b** calibrated Brillouin-shift dependence of normalized signal

Figure 8 shows the experimental result. Figure 8a gives the measured data of Brillouin shift at different temperatures. The dots with error bars are the measured data. Each dot is the average of 200 measurements. In the measured normalized signal, the values were larger than 1 at lower temperatures, since the beam splitter used (BS in Fig. 7) was not a strict 1 : 1 splitter; also, at low temperature a small Brillouin shift forms a small overlap area between the Brillouin line and the absorption line of the iodine cell. Figure 8b gives the calibrated result of the normalized signal vs. Brillouin shift, which we can use to determine the Brillouin shift in water by measuring the normalized intensity. The calibration was made using our previous experimental measurements on Brillouin scattering [12]. Here, it should be pointed out that the function of Fig. 8b is a calibration, but it is based on the specific absorption cells used at certain pressures and temperatures. However, it is easy to calibrate the normalized signal for different measuring conditions.

5 Statistical error of the technique

Assuming that only the shot noise is considered, the statistical error is related to the signal-to-noise ratio of the system as [16]

$$\mathrm{SNR} = N_{\mathrm{pe}}/\sqrt{N_{\mathrm{pe}}} = \sqrt{N_{\mathrm{pe}}}\,.$$

Then, the statistical error in Brillouin shift can be expressed as

$$\Delta\nu_{\mathrm{B}} = \alpha\Gamma_{\mathrm{B}}/\mathrm{SNR} = \alpha\Gamma_{\mathrm{B}}/\sqrt{N_{\mathrm{pe}}}\,, \tag{6}$$

where α is a factor of statistical uncertainty; it has a value larger than unity. In general, its value can be chosen as $\alpha < 4$. In this paper, we choose it as $\alpha = 3$. Figure 9 gives the statistical error in Brillouin shift. It is clear that the statistical error will be smaller when the energy of the laser output is higher, because more photon numbers from the laser would induce more Brillouin photo-electrons (which gives a larger value of N_{pe}), and will result in a higher signal-to-noise ratio. From Fig. 9, in the temperature range used, $\Delta\nu_{\mathrm{B}}$ of the measurements is about 20 MHz, and thus the relative statistical error is less than 2%.

The details of the discussion of the statistical uncertainty are more complicated, and will be presented in another paper.

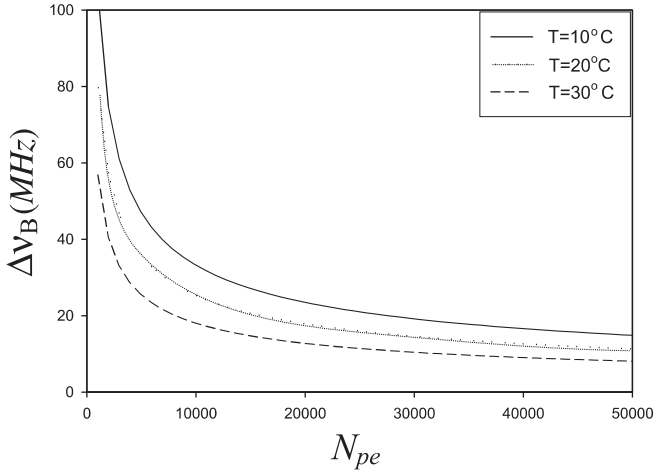

FIGURE 9 Statistical error in Brillouin shift

ACKNOWLEDGEMENTS The authors thank the National Natural Science Foundation of China (Grant Nos. 69988001 and 10274006) and the National Advanced Technology Program (Grant No. 2002AA633110) for financial support. Also, the authors would like to thank Prof. E.S. Fry and Dr. J.W. Katz of Texas A&M University, USA for helpful discussions.

REFERENCES

1 J.A. Gelbwachs: IEEE J. Quantum Electron. **QE-24**, 1266 (1988)
2 G. Yang, R.I. Billmer, P.R. Herczfeld, V.M. Contarino: Opt. Lett. **22**, 414 (1997)
3 C.L. Korb, B.M. Gentry, C.Y. Weng: Appl. Opt. **31**, 4202 (1992)
4 C.L. Korb, B.M. Gentry, X. Li: Proc. SPIE **2310**, 206 (1994)
5 J.S. Friedman, C.A. Tepley, P.A. Castleberg, H. Roe: Opt. Lett. **22**, 1648 (1997)
6 P. Piironen, E.W. Eloranta: Opt. Lett. **19**, 234 (1994)
7 J.N. Forkey, W.R. Lempert, R.B. Miles: Appl. Opt. **36**, 6729 (1997)
8 J.G. Hirschberg, J.D. Byrne, A.W. Wouters, G.C. Boyton: Appl. Opt. **23**, 2624 (1984)
9 J.G. Hirschberg, J.D. Byrne: Proc. SPIE **489**, 270 (1984)
10 D.J. Collins, J.A. Bell, R. Zanoni, I.S. McDermid, J.B. Brecknridge, C.A. Sepulveda: Proc. SPIE **489**, 247 (1984)
11 G.D. Hickman, J.M. Harding, M.C. Garnes, A. Pressman, G.W. Kattawar, E.S. Fry: Remote Sens. Environ. **36**, 165 (1991)
12 D. Liu, J. Xu, R. Li, R. Dai, W. Gong: Opt. Commun. **203**, 335 (2002)
13 D.A. Leonard, H.E. Sweeney: Proc. SPIE **925**, 407 (1988)
14 I.L. Fabelinskii: *Molecular Scattering of Light* (Plenum, New York 1968)
15 I.L. Fabelinskii: Prog. Opt. **37**, 97 (1997)
16 J.W. Goodman: *Statistical Optics* (Wiley, New York 1985) pp. 470–520